Published in final edited form as:
Osteoporos Int. 2012 July ; 23(7): 1977–1985. doi:10.1007/s00198-011-1851-3.

Assessment of Technical and Biological Parameters of Volumetric Quantitative Computed Tomography in the Foot: A Phantom Study

Kirk E. Smith[a], **Bruce R. Whiting**[b], **Gregory G. Reiker**[a], **Paul K. Commean**[a], **David R. Sinacore**[c], and **Fred W. Prior**[a]

[a]Electronic Radiology Laboratory, Mallinckrodt Institute of Radiology, Washington University School of Medicine, St. Louis, MO

[b]University of Pittsburgh, Department of Radiology, Pittsburgh, PA

[c]Applied Kinesiology Laboratory, Program in Physical Therapy, Washington University School of Medicine, St. Louis, MO

Abstract

Few studies exist for bone densitometry of the whole foot. A phantom study demonstrated the sources of error and necessary controls for accurate quantitative computed tomography of the foot. A loss in bone mineral density in the small foot bones may be an early indicator of diabetic foot complications.

Purpose—Volumetric quantitative computed tomography (vQCT) facilitates assessment of pedal bone osteopenia, which in the presence of peripheral neuropathy may well be an early sign of diabetic foot deformity. To date, sources and magnitudes of error in foot vQCT measurements have not been reported.

Methods—Foot phantoms were scanned using a 64-slice CT scanner. Energy (kVp), table height, phantom size and orientation, location of “bone” inserts, insert material, location of calibration phantom, and reconstruction kernel were systematically varied during scan acquisition.

Results—Energy (kVp) and distance from the isocenter (table height) resulted in relative attenuation changes from −5% to 22% and −5% to 0%, respectively, and average bone mineral density (BMD) changes from −0.9% to 0.0% and −1.1% to 0.3%, respectively, compared to a baseline 120 kVp scan performed at the isocenter. BMD compared to manufacturer specified values ranged on average from −2.2% to 0.9%. Phantom size and location of bone-equivalent material inserts resulted in relative attenuation changes of −1.2% to 1.4% compared to the medium sized phantom.

Conclusion—This study demonstrated that variations in kVp and table height can be controlled using a calibration phantom scanned at the same energy and height as a foot phantom; however, error due to soft tissue thickness and location of bones within a foot cannot be controlled using a calibration phantom alone.

*Corresponding Author: Kirk E. Smith, B.S., Address: Mallinckrodt Institute of Radiology, Washington University School of Medicine, 510 South Kingshighway Blvd, Campus Box 8131, St. Louis, MO 63110, USA, Telephone: (314) 362-8474, Fax: (314) 362-6971, smithki@mir.wustl.edu.

Conflict of Interest: No Disclosures

Keywords

Foot; Bone Mineral Density; Quantitative Computed Tomography; Diabetes; Neuropathic Charcot's Arthropathy; Phantom

Introduction

Neuropathic Charcot's arthropathy (NCA) is a debilitating complication of diabetes mellitus and peripheral neuropathy (DM+PN), which results in the highest incidence of amputation [1] among people with diabetes. NCA is characterized by a swollen, temperature-elevated foot, with an accompanying fracture or dislocation of one or more pedal bones [2]. Though the pathogenesis of NCA is incompletely understood, it is generally believed that distal symmetrical polyneuropathy leads to a poorly regulated blood flow and bone resorption, which places a foot at risk for an acute Charcot event [3]. Pedal bone osteopenia, as characterized by low bone mineral density (BMD) of one or more foot bones in the presence of DM+PN, may well be the earliest sign of the onset of NCA. Midfoot bones and joints appear to be especially susceptible, as tarsal-metatarsal bones (Lisfranc joints) are the most common site of Charcot destruction [4,5]. Early detection of prognostic indicators of NCA in pedal bones may lead to early intervention and better outcomes from this devastating condition [6]. When using bone densitometry to quantify BMD of Charcot afflicted feet, it is important to discern changes in BMD that are attributable to actual change in bone structure from measured changes in BMD that are simply a byproduct of swelling, foot orientation, or scanning technique.

QCT in the spine has been well documented [7-9], but few studies exist for the foot. QCT may provide valuable information regarding BMD of all the foot bones; however, for proper interpretation it is important to understand measurement properties, the potential sources of variation in the measurement, and how to control parameters to achieve optimal results and accurate interpretation. QCT involves converting grayscale values that are calibrated in Hounsfield Units (HU) [10], to values of BMD through use of a calibration reference phantom that has a known concentration of bone surrogate material within a collagen surrogate substrate [11,12]. Factors relating to the scan acquisition, such as beam hardening in the X-ray energy spectrum, can influence the measured HU values, resulting in different values for the same tissue in different positions in the foot. Also, different scanners or the same scanner at different times could give varying results (although this effect is greatly diminished by modern scanner calibration techniques). Errors in HU values due to imaging technique and errors from the reference calibration object contribute to errors in estimates of BMD from QCT.

The purpose of this study is to determine the influence that technical and biological parameters have on vQCT of the foot, and to examine issues involved in converting HU to BMD (in units of mgHA/cm^3). Beam spectrum is studied by varying the energy (kVp) and beam hardening is studied by varying the size, location, orientation, and composition of a foot phantom within the polychromatic, non-uniform X-ray fan beam. In order to isolate the effects of different elemental compositions, the objects studied consisted of homogenous materials, without any microstructure such as found in biological tissues. The method of HU to BMD (mgHA/cm^3) conversion, using scans of a reference phantom calibrated over the trabecular range (0 to 200 mgHA/cm^3), was studied by scanning the calibration phantom both in and out of the field of view (FOV) of the test object (foot phantom), and by testing phantoms with densities in the cortical bone range. We discuss the implications these results have on our existing vQCT protocol for examining diabetic, neuropathic feet with and without acute NCA.

Materials and Methods

Phantoms

A commercial phantom (QCT-Bone Mineral™ phantom; Image Analysis, Inc., Columbia, Kentucky, Serial No. 4225) has been employed in our human subjects research protocol to generate conversion equations to map HU to BMD. The Image Analysis (IA) calibration phantom consists of three embedded rods (20 mm in diameter) with different concentrations of calcium hydroxyapatite embedded in a water-equivalent polymer housing, with dimensions of 300 mm × 152 mm × 32 mm. These rods consisted of the specified concentrations of 50.0, 100.0 and 200.0 mgHA/cm^3 with an accuracy of +/−0.5%. This phantom, shown in Figure 1 **(bottom of A and B)**, was designed for QCT studies of trabecular regions of bones and has a maximum concentration of 200 mgHA/cm^3. We used the IA calibration phantom for our vQCT study; however, other calibration phantoms could be used instead.

Three foot phantoms were constructed in our machine shop from a block of Solid Water™ (Gamex-rmi, Madison, WI), an accepted CT surrogate material for soft tissue. These phantoms had cavities machined to accept five cylindrical, 60 mm long inserts, one with a diameter of 19 mm and four with diameters of 9 mm, as shown in Figure 1 **(top of A and B)**. The machining process assured a tight fit of the inserts to minimize any air gap. Inserts of different materials were constructed to represent different bone densities. The only difference in the three foot phantoms was the amount of soft tissue surrounding the inserts. The height-width dimensions of the small, medium, and large phantoms were 3.81 cm × 7.62 cm, 5.715 cm × 10.16 cm, and 8.89 cm × 12.065 cm, respectively. The size differences in the foot phantoms were chosen to test the effects of swelling and soft tissue differences on measured attenuation (HU).

Inserts

To test the variation in BMD values over the experimental conditions, inserts containing hydroxyapatite crystals embedded within a soft tissue surrogate (epoxy resin) substrate were custom ordered from QRM (QRM GmbH, Moehrendorf, Germany). The inserts were designed and manufactured to fit within the three foot phantoms and to cover the HU range from water to cortical bone. The QRM inserts were used to test the linearity of the CT scanner, to test the accuracy of the HU to BMD conversion in the cortical range when extrapolating values from the IA calibration phantom, and to test the ability of a BMD calibration scan to control for variation in scanning technique and foot morphology (soft tissue thickness and bone location within soft tissue). The QRM inserts consisted of the specified concentrations of 0.0, 51.54, 99.52, 206.44, 400.22, 816.3, and 1024.05 mgHA/cm^3. One insert of each HA concentration was purchased in the 9 mm × 60 mm size and an additional two inserts with specified concentrations of 0.0 and 1024.05 mgHA/cm^3 were purchased in the larger 19 mm × 60 mm size. We will refer to these inserts as HA0, HA50, HA100, HA200, HA400, HA800, and HA1000. Four of the QRM inserts (HA0, HA50, HA100, and HA200) approximated concentrations of HA used in the IA calibration phantom. To test the effects of insert location and foot phantom orientation, five additional inserts of polychlorotrifluoroethylene (PCTFE; a surrogate material for cortical bone) were machined to tightly fit within the cavities of the foot phantoms.

Image Acquisition

For scanning purposes, a holder was manufactured, which attached to the scanner table and incorporated a “split-ball” vise (PanaVise Products, Inc., Reno, NV), to position (tilt, turn, and rotate) a phantom in an open gantry with no other objects, including the scanner bed, present in the scanner field of view. The holder attached directly to the scanner's mounting

bracket that is used to hold a quality assurance phantom during daily scanner calibration. All scans were performed on a 64-slice Siemens Somatom Definition CT scanner (Siemens Medical Solutions, Forchheim, Germany). A baseline protocol was defined as 120 kVp, 2 rotations per second, spiral mode, table feed of 38.4 mm per rotation, 64 × 0.6 mm, pitch of 1, 220 effective mAs, 308 mm FOV, 160.5 mm table height (phantom centered at the scanner isocenter), 0 degrees phantom inclination, and medium-sized foot phantom. A high-resolution kernel (B70f) was used to reconstruct the images. Parameters that were varied about this baseline included: energy (kVp), distance from isocenter (table height), amount of soft tissue surrounding inserts (foot phantom size), the angle of foot orientation during scanning (angle), the insert material, the location of the inserts within the phantom, the location of the calibration phantom during scan acquisition, and the reconstruction kernel. For each scan of the foot phantom, a separate scan of the IA calibration phantom was performed at the same settings with the exception of the scan where the IA calibration phantom was scanned while in contact with the foot phantom.

Placement of IA Calibration Phantom

To test the effect of having the IA calibration phantom in contact with the foot during scanning, as recommended by the phantom manufacturers for spinal QCT, compared to performing a separate scan of the IA calibration phantom at the same table height as the foot, we performed a scan using the medium-sized foot phantom, with QRM inserts, in the following order: 1) HA0, large insert; 2) HA200; 3) HA400; 4) HA800; 5) HA1000. The IA calibration phantom was clamped into the mounting vice and leveled. The medium sized foot phantom was placed atop the IA calibration phantom, in direct contact, and the scanner table raised until the center of the foot phantom was positioned at the isocenter, as determined by the positioning lasers on the scanner. A 3 cm long scan was then performed through the central region of the phantoms using the baseline scanning parameters. The IA calibration phantom was removed, and the foot phantom was scanned alone. The IA calibration phantom was then repositioned at the isocenter and also scanned alone.

CT Scan Linearity and Stability

To test the linearity of the CT scanner across the density range from trabecular to cortical bone, a scan of five QRM inserts HA0, HA200, HA400, HA800, and HA1000 was performed at the isocenter. To test the stability of the CT scanner, the IA calibration phantom was repositioned in the holder at the isocenter, and a scan was performed. This scan was compared to the earlier IA calibration scan performed at the isocenter.

Test of X-ray Tube Energy on HU and BMD

To test the effect of X-ray tube energy on HU and BMD, four scans of the medium-sized foot phantom were performed at 80 kVp, 100 kVp, 120 kVp, and 140 kVp using the baseline scanning parameters. The foot phantom was not repositioned between scans. Scans of the IA calibration phantom alone (at the isocenter) were performed at 80 kVp, 100 kVp, 120 kVp, and 140 kVp. A 140 kVp scan is not a good option for QCT of the foot due to higher dose; however, we include it in our study as it is available for extremity scanning and provides an additional reference point.

Test of Distance from Isocenter on HU and BMD

To test the effect of object distance relative to the isocenter on HU and BMD, the table was lowered 134.5 mm, representing the lowest position at which a foot scan could occur within the gantry, and a scan performed of the medium-sized foot phantom using the baseline scanning parameters. The table was then raised 68 mm to represent a mid-location (66.5 mm from the isocenter) within the gantry, and a scan was performed with all other imaging and

foot phantom parameters left unchanged. The IA calibration phantom scans were also performed at these table heights.

Impact of Foot Phantom Size and Insert Location on HU

As a test of bone location and soft tissue thickness on HU values, and thus on BMD, five bone inserts of identical material (PCTFE) were placed in the small, medium, and large foot phantoms and scanned using the default scanning parameters.

Effect of Foot Phantom Orientation

To test the effect of placing a foot at a 45 degree angle during scan acquisition, the medium-sized foot phantom was scanned at 0 degrees of inclination and then again at 45 degrees of inclination. For these scans, the five inserts were all made of identical material (PCTFE).

Effect of Reconstruction Kernel

To test the effect of CT reconstruction kernel on BMD values, the x-ray projection data for the default scan was reconstructed using Siemens B30f, B35f, B40f, and B70f kernels. The corresponding IA calibration phantom scan data were reconstructed using the same kernels and were used to construct kernel specific calibrations to convert HU to values of BMD.

Measurements

Reconstructed image sets were saved in DICOM format, transferred to a standalone workstation, and loaded into the Analyze software system [13] for region of interest (ROI) measurements. For the three different-sized foot phantoms, five ROIs were defined, i.e., one region for each insert. These regions of interest were defined on 34 contiguous slices covering 2.04 mm in length. For the large insert, an 11.6 mm diameter circular ROI was defined, and for the small insert locations, 3.9 mm diameter circular ROIs were defined **(**Figure 1B**, top)**. The ROIs were sized to exclude edge effects. For the four component IA calibration phantom, four ROIs were defined using 11.6 mm diameter circular ROIs **(**Figure 1B**, bottom)**. For scans of the foot phantom that contained the QRM inserts and for scans of the IA calibration phantom, the same image mask was used to measure all scans. For the scans where the table positions were adjusted, simple translations were performed to align ROIs within the inserts. For the scans testing the angle of foot orientation and foot phantom size effects, where only the PCTFE inserts were used, the ROIs were similarly defined except they were defined individually for each scan, as the foot phantoms were moved between scans and the translations and rotations necessary to precisely align a predetermined ROI in three-dimensions could not be easily determined.

The IA calibration phantom scans, acquired under the same conditions as the foot phantoms being examined, were used to convert the measured HU values of the QRM inserts into corresponding BMD values (mgHA/cm^3).

Results

Placement of IA Calibration Phantom

The effects of scanning the medium-sized foot phantom, with and without the IA calibration phantom in the FOV, are given in Table 1. The calibrated BMD values, using the previously described method, vary from the specified values (as given by QRM in mgHA/cm^3) by −2.2% to 1.9% for the QRM inserts with the IA calibration phantom in the FOV, while they varied by −1.6% to 0.9% without the IA calibration phantom in the FOV.

In order to reduce the nonlinear HU effects on the foot phantom inserts, caused by additional mass in the FOV and inconsistent placement of the IA calibration phantom relative to the foot phantom, all subsequent scans of the foot phantoms were performed without the IA calibration phantom in the FOV.

CT Scan Linearity and Stability

For the QRM inserts in the medium foot phantom, there is a good linear fit, R^2=0.9998, for the BMD values versus the measured HUs. For the two scans of the IA calibration phantom within a single scanning session, the measured HU values for the three embedded rods varied from −0.9% to 0.4% from the first to the second. The accuracy of the IA calibration, extrapolated through cortical bone values, for the baseline protocol is shown in a Bland-Altman [14] plot (Figure 2).

Test of X-ray Tube Energy on HU and BMD

For the medium-sized foot phantom, the relative attenuation values (HU) of the QRM inserts vary by −5% to 22% for 140 kVp to 80 kVp, respectively, compared to the 120 kVp results. The calibrated BMD values for the inserts at the different energy levels are given in Table 2, along with the mgHA/cm^3 values specified by QRM for each insert type used. The average percent differences are shown at each energy level, as compared to both the default 120 kVp scan values and the QRM specified values. For each QRM insert used, the calibrated BMD values differ on average by −0.9% to 0.0% from the values at 120 kVp and differ on average by −2.0% to 0.9% from the values as specified by QRM.

Since 120 kVp reliably produced acceptable image quality and is specified in the clinical protocol for lower extremities, all subsequent scans of the phantoms were performed at this energy level.

Test of Distance from Isocenter on HU and BMD

Varying the table height of an object places it at a different distance from the isocenter, causing the effective energy of the beam to change due to the bow-tie filter of the CT scanner [15]. The observed effect of table height is that high attenuation materials trend to lower HU values as the distance from the isocenter increases, changing relative attenuation by as much as −4.8% for the four QRM inserts used. The calibrated BMD values for the medium-sized foot phantom with QRM inserts, at three different table heights, are given in Table 3, with the average percent differences from the calibrated BMD values at the isocenter for each of the QRM inserts used and the average percent differences of the calibrated BMD values from the specified values for each of the QRM inserts.

Impact of Foot Phantom Size and Insert Location on HU

The variations of the measured HU values of the five PCTFE inserts with the small, medium, and large foot phantoms are shown in Figure 3. For the small- and large-sized foot phantoms, the relative attenuations of the inserts changed by −1.2% to 1.4% as compared to those in the medium-sized foot phantom. For a given foot phantom, the relative attenuations of the different insert locations changed by 0.5% to 3.7% as compared to the respective insert located at the center. All data distributions were normally distributed (Shapiro-Wilk W test $p > 0.05$) and variances were equally distributed (O'Brien, Brown-Forsythe, Levene, and Bartlett tests $p > 0.05$). Using paired t tests, and a Bonferroni corrected p value ($p = 0.005$), significant differences were found between 7 of 10 paired locations (1-2; 1-3; 1-4; 3-4; 5-2; 5-3; 5-4). An analysis of variance test found no differences among phantom size group means ($p > 0.05$); however, the HU values tend to increase as the size of the foot phantom decreases.

Effect of Foot Phantom Orientation

For the medium-sized foot phantom, with five identical simulated-bone inserts (PCTFE), the measured foot phantom effective heights and relative attenuation values of the center insert are given, as follows: 56.9 mm and 1350.3 HU at 0 degrees; 78.0 mm and 1349.6 HU at 45 degrees. The inclination of the foot phantom at 45 degrees effectively changed the cross-sectional thickness of the soft tissue, elongating it by a factor of the reciprocal of the cosine of the angle of inclination.

Effect of Reconstruction Kernel

For the medium-sized foot phantom the results are given in Table 4. The B70f and B35f kernels resulted in mean values of mgHA/cm^3 that were closer to the values specified by QRM for the inserts than did either the B30f or B40f kernel. The standard deviations for the B30f, B35f, and B40f kernels were comparable to each other and were much lower than the standard deviation of the B70f kernel.

Discussion

The typical application of QCT has been analysis of trabecular bone in the spine, hip, proximal femur, and forearm, using BMD calibration phantoms manufactured with known concentrations of hydroxyapatite in a range of 0 to 200 mgHA/cm^3 (approximately 0 to 250 HU), which represents the range for trabecular bone with clinical CT [16,17]. Cortical bone, however, ranges upward of 900 HU [10], and existing BMD phantoms do not calibrate this upper range. To confirm that calibration, multiple points spanning the entire range should be used. This study demonstrates that the 64-slice Siemens Somatom Definition CT scanner used in this study has a linear relationship between HU and mgHA/cm^3 across the trabecular bone to cortical bone range, and that extrapolating cortical BMD values from a trabecular BMD calibration phantom gives good results. Using a phantom with lower BMD values, such as found in trabecular BMD calibration phantoms, avoids beam hardening errors that result when dense objects are scanned. We would anticipate that other modern multi-row CT scanners would perform similarly and would likewise exhibit the general characteristics described below.

The most common modality for obtaining and reporting BMD values is DXA, which provides an areal measurement in mg/cm^2. BMD values reported in this manner are often denoted as aBMD to distinguish them from volumetric measures of BMD. Measures of BMD by DXA have their own set of limitations, as discussed by Bolotin, making the modality of limited value for comparing results to QCT-derived measures of BMD [18], particularly for the small bones of the foot.

While there have been no reported systematic investigations of sources of error and correction techniques for vQCT of the foot, Bligh et al. used a phantom study to investigate multi-row vQCT parameters on the precision of BMD and reported precision estimates of 1.4% when scanning parameters were controlled [19]. Bligh et al. reported an upward trend of BMD values as the table height moved the patient phantom away from the isocenter. We found a reduction in HU values as the foot phantom was moved away from the isocenter; however, the calibration of HU to BMD controlled for the HU variation, and no upward trend in BMD values was noted. The reduction in HU as the object moves away from the isocenter is an effect of the bow-tie filter used to minimize patient dose. The design of the filter is intended to equalize beam flux through tissue thickness differences in the torso, and it attenuates more flux at the limits of the field of view than in the center. In the case of foot scanning, the bow-tie filter is not optimized as the foot has very little soft tissue compared to the torso and is much smaller in size. The Bligh et al. study was based on vQCT scans of

vertebrae with the BMD calibration phantom placed under the “patient” phantom during the acquisitions. The upward effect of BMD could be related to both the bow-tie filter and beam hardening artifact resulting from the reference standard being in the field of view during scanning. Comparison of vQCT derived BMD to known values in phantoms was not performed to assess accuracy of measurements as Bligh et al. focused strictly on precision. Our study identifies sources of error found with vQCT of feet and shows which errors can be controlled through scanning technique and which errors still remain. While these errors are specific to foot scanning, the same principles can be applied to vQCT in general.

The current recommendation for QCT of the spine is to scan the BMD calibration phantom in the FOV with the object under examination [16]. This locates the BMD calibration phantom at approximately the same distance from the isocenter as the spine and has similar attenuation due to beam hardening. In the case of foot scanning with vQCT, our data suggests the optimal placement of a BMD calibration phantom may be outside the field of view of the foot being scanned. Further studies of BMD calibration phantom placement during foot scanning would be needed to confirm this observation. The foot is a relatively small object, and relative HU values are more variable with positioning.

Our current scanning protocol utilizes an energy setting of 120kVp, the standard-of-care diagnostic setting, when evaluating lower extremities with CT. Other workers have reported that using the lowest energy setting available is preferred for QCT scanning of the spine. Our study demonstrates that similar BMD values are obtained at different energy settings when a BMD calibration phantom is utilized. Our data also show that using a lower energy setting yields a greater difference in HUs between objects having different concentrations of HA. If thresholding is employed to discriminate trabelcular bone from marrow or if thin cortical edges make it difficult to segment a bone from surrounding soft tissues, then a lower kVp may provide better separation of HU for those purposes.

With any phantom study, there are limitations when applying the findings to research and ultimately to clinical practice. The “foot” phantoms modeled soft tissue as a uniform water-equivalent material and modeled bone as a mixture of calcium hydroxyapatite within an epoxy substrate. The bone insert design made no attempt to model trabecular geometry. In clinical practice, the current state of the art clinical CT scanners do not have sufficient spatial resolution to fully resolve trabecular structure or thin cortical shells and results may be influenced due to partial volume effects [20].

Both soft tissue and bone reconstruction kernels are used in clinical QCT [16]. A soft tissue reconstruction kernel results in an image with less noise and may be preferred for typical spinal QCT evaluation. With the increased spatial resolution afforded by multi-detector CT, some investigators have begun to assess bone structure in conjunction with BMD. In these cases, a high spatial reconstruction kernel was used to better delineate structure [21]. Typically, a manufacturer's kernel design is not publicly available and effects of kernel selection on HU must be determined empirically. In our phantom study, we found that a B70f kernel provided accurate results for a volumetric analysis of BMD for small bones in the foot. For a sub-regional analysis or 2D analysis of foot BMD, a reconstruction kernel with a lower standard deviation would be desirable. For a longitudinal study, the choice of kernel should be selected based on the parameters of interest, and then not changed. CT scanning also utilizes ionizing radiation, but the effective dose in the ankle and foot is about 0.07 mSv, which is less than a routine posteroanterior chest radiograph [22]. For our investigation of BMD in feet, we used a single CT scanner. For a multi-center trial, differences between scanners would need to be examined more thoroughly.

Ideally, for forefoot and midfoot scanning, we would align the long axis of the foot perpendicular to the scan plane; however, most subjects with diabetes mellitus enrolled in our studies have a limited range of motion about the ankle. For whole foot scanning, where the calcaneus is imaged, a 45 degree alignment provides the least interaction between the tibia/fibula and the calcaneus. Therefore, we scan the foot at a 45 degree angle of inclination.

We did not test the variation of tube current, as theoretically that should have little effect on mean HU, and tests by other workers have confirmed this [23]. The experiments and results reported in this paper confirm that our scanning technique will control for sources of error to the best extent possible.

Some biological parameters cannot be controlled for during scanning, and these parameters may affect measured BMD values. These include swelling and location of a bone within the foot. We have shown that bones of similar concentrations of HA can have different HU depending on location, with bones in the central portion of the foot having lower values than bones located medially or laterally. The most likely cause of this artifact is that beam hardening correction is optimized for water and not for dense objects as used in this study. Use of the IA calibration phantom does not control for this source of error. This variation should have little effect for longitudinal studies comparing the same subject over time, as the location of the bones within the soft tissue and relationship to surrounding bones remains relatively fixed. We also demonstrated an inverse relationship between amount of soft tissue and HU of bone. This finding does have an impact on longitudinal studies; therefore, a decrease in BMD in the presence of soft tissue swelling should be considered with caution if correction methods are not employed.

Quantifying the variation in HU and BMD for a given tissue due to technical and biological factors provides an estimate of error in a measurement, but more importantly, understanding the source of the variation allows for controls and corrections to be implemented to achieve the best possible reliability and accuracy for a particular patient's foot. One possible correction technique that could be utilized to minimize the impact of swelling and the location of a bone within the foot would follow the method of Zerhouni et al. for lung nodule assessment [24]. This would involve having a series of foot-shaped phantoms of different sizes and inserts. An appropriate BMD calibration phantom, matching the general size of a patient's foot, would be selected, positioned, and scanned to correct for size and location of bones within a foot. This, however, may not be a clinically tenable solution. An alternative method of correction would utilize a synthetic image formation model to compute corrections. A CT image of the foot would be post-processed in a mathematical model of the CT system, where the beam spectrum and bow-tie filter were specified and the foot treated as a two component bone and soft tissue model, with corrections calculated based on what the actual values should be. We are working on developing such a mathematical model and believe errors due to swelling and location of a bone within a foot can likely be reduced. Measurement data (sinograms) are now being archived from patient scans, allowing the possibility of retrospective reconstructions as we develop improved processing techniques.

Conclusions

Current efforts to identify candidate prognostic and therapeutic biomarkers for NCA based on vQCT [25] are heavily dependent on an understanding of the accuracy and precision of BMD measurements. These measurements are comprised of two components, the inherent accuracy of the imaging technique discussed here and the error introduced by the image analysis process [26].

This study demonstrated that HU variations due to energy (kVp) and distance from the isocenter (table height) can be controlled when converting to BMD by using an IA calibration phantom scanned at the same kVp and table height as a foot phantom; however, HU variations due to soft tissue thickness and the location of bones within a foot cannot be fully controlled when converting to BMD by using an IA calibration phantom alone. For the best results during foot scanning, we recommend aligning the center of the foot at the isocenter, positioning the foot at a fixed angle of inclination, and using the same kVp setting for all scans. While these results are manufacturer and scanner specific due to scanner specific field inhomogeneities, it is likely that the technical and biological parameters described in this study would produce similar effects for vQCT foot scanning using other modern CT scanners. QCT in the feet may be useful as both a clinical and research option for assessing risk and response to treatment for diabetic foot disease.

Acknowledgments

Funding for this project was provided by the National Institutes of Health, National Institute of Diabetes, Digestive and Kidney Diseases (1 R21 DK079457-03). We thank Tim Street, CT technologist within the Clinical Center for Imaging Research (CCIR) for his help with CT image acquisition for this project. The CCIR is supported in part from the National Center for Research Resources (NCRR), a component of the National Institutes of Health (NIH) (1 UL1 RR024992-01). We also thank Dr. Charles Hildebolt for statistical assistance.

References

1. Sohn MW, Stuck RM, Pinzur M, Lee TA, Budiman-Mak E. Lower-extremity amputation risk after charcot arthropathy and diabetic foot ulcer. Diabetes Care. 2010; 33(1):98–100. [PubMed: 19825822]
2. Sinacore DR, Hastings MK, Bohnert KL, Fielder FA, Villareal DT, Blair VP 3rd, Johnson JE. Inflammatory osteolysis in diabetic neuropathic (charcot) arthropathies of the foot. Phys Ther. 2008; 88(11):1399–1407. [PubMed: 18801857]
3. Rajbhandari SM, Jenkins RC, Davies C, Tesfaye S. Charcot neuroarthropathy in diabetes mellitus. Diabetologia. 2002; 45(8):1085–1096. [PubMed: 12189438]
4. Brodsky, JW. The Diabetic Foot Surgery of the Foot and Ankle. 6. Mosby Year Book; St. Louis: 1993.
5. Schon LC, Weinfeld SB, Horton GA, Resch S. Radiographic and clinical classification of acquired midtarsus deformities. Foot Ankle Int. 1998; 19(6):394–404. [PubMed: 9677084]
6. Chantelau E, Kimmerle R, Poll LW. Nonoperative treatment of neuro-osteoarthropathy of the foot: do we need new criteria? Clin Podiatr Med Surg. 2007; 24(3):483–503. ix. [PubMed: 17613387]
7. Genant HK, Ettinger B, Cann CE, Reiser U, Gordan GS, Kolb FO. Osteoporosis: assessment by quantitative computed tomography. Orthop Clin North Am. 1985; 16(3):557–568. [PubMed: 3892413]
8. Gluer CC, Reiser UJ, Davis CA, Rutt BK, Genant HK. Vertebral mineral determination by quantitative computed tomography (QCT): accuracy of single and dual energy measurements. J Comput Assist Tomogr. 1988; 12(2):242–258. [PubMed: 3351039]
9. Lang TF, Augat P, Lane NE, Genant HK. Trochanteric hip fracture: strong association with spinal trabecular bone mineral density measured with quantitative CT. Radiology. 1998; 209(2):525–530. [PubMed: 9807584]
10. Hounsfield GN. Nobel Award address. Computed medical imaging. Med Phys. 1980; 7(4):283–290. [PubMed: 6993911]
11. Cann CE, Genant HK. Precise measurement of vertebral mineral content using computed tomography. J Comput Assist Tomogr. 1980; 4(4):493–500. [PubMed: 7391292]
12. Kalender WA. A phantom for standardization and quality control in spinal bone mineral measurements by QCT and DXA: design considerations and specifications. Med Phys. 1992; 19(3):583–586. [PubMed: 1508094]

13. Robb RA. The biomedical imaging resource at Mayo Clinic. IEEE Trans Med Imaging. 2001; 20(9):854–867. [PubMed: 11585203]

14. Bland JM, Altman DG. Statistical methods for assessing agreement between two methods of clinical measurement. Lancet. 1986; 1(8476):307–310. [PubMed: 2868172]

15. Boone JM. Method for evaluating bow tie filter angle-dependent attenuation in CT: theory and simulation results. Med Phys. 37(1):40–48. [PubMed: 20175464]

16. Engelke K, Adams JE, Armbrecht G, Augat P, Bogado CE, Bouxsein ML, Felsenberg D, Ito M, Prevrhal S, Hans DB, Lewiecki EM. Clinical use of quantitative computed tomography and peripheral quantitative computed tomography in the management of osteoporosis in adults: the 2007 ISCD Official Positions. J Clin Densitom. 2008; 11(1):123–162. [PubMed: 18442757]

17. Griffith JF, Genant HK. Bone mass and architecture determination: state of the art. Best Pract Res Clin Endocrinol Metab. 2008; 22(5):737–764. [PubMed: 19028355]

18. Bolotin HH. DXA in vivo BMD methodology: an erroneous and misleading research and clinical gauge of bone mineral status, bone fragility, and bone remodelling. Bone. 2007; 41(1):138–154. [PubMed: 17481978]

19. Bligh M, Bidaut L, White RA, Murphy WA Jr, Stevens DM, Cody DD. Helical multidetector row quantitative computed tomography (QCT) precision. Acad Radiol. 2009; 16(2):150–159. [PubMed: 19124100]

20. Hangartner TN, Short DF. Accurate quantification of width and density of bone structures by computed tomography. Med Phys. 2007; 34(10):3777–3784. [PubMed: 17985623]

21. Bousson V, Le Bras A, Roqueplan F, Kang Y, Mitton D, Kolta S, Bergot C, Skalli W, Vicaut E, Kalender W, Engelke K, Laredo JD. Volumetric quantitative computed tomography of the proximal femur: relationships linking geometric and densitometric variables to bone strength. Role for compact bone. Osteoporos Int. 2006; 17:855–864. [PubMed: 16547689]

22. Biswas D, Bible JE, Bohan M, Simpson AK, Whang PG, Grauer JN. Radiation exposure from musculoskeletal computerized tomographic scans. J Bone Joint Surg Am. 2009; 91(8):1882–1889. [PubMed: 19651945]

23. Tanaka C, Ueguchi T, Shimosegawa E, Sasaki N, Johkoh T, Nakamura H, Hatazawa J. Effect of CT acquisition parameters in the detection of subtle hypoattenuation in acute cerebral infarction: a phantom study. AJNR Am J Neuroradiol. 2006; 27(1):40–45. [PubMed: 16418353]

24. Zerhouni EA, Boukadoum M, Siddiky MA, Newbold JM, Stone DC, Shirey MP, Spivey JF, Hesselman CW, Leo FP, Stitik FP, et al. A standard phantom for quantitative CT analysis of pulmonary nodules. Radiology. 1983; 149(3):767–773. [PubMed: 6647853]

25. Prior, F.; Commean, P.; Ju, T.; Hastings, M.; Hildebolt, C.; Sinacore, D. Developing a Biomarker for Neuropathic Arthropathy in Diabetic Patients. In: Xplore, I., editor. Life Science Systems and Applications Workshop. Bethesda, MD: Nov 8-9. 2007 p. 13-16.

26. Commean PK, Kennedy JA, Bahow KA, Hildebolt CF, Liu L, Smith KE, Hastings MK, Ju T, Prior FW, Sinacore DR. Volumetric quantitative computed tomography measurement precision for volumes and densities of tarsal and metatarsal bones. Journal of Clinical Densitometry. 2011 Accepted.

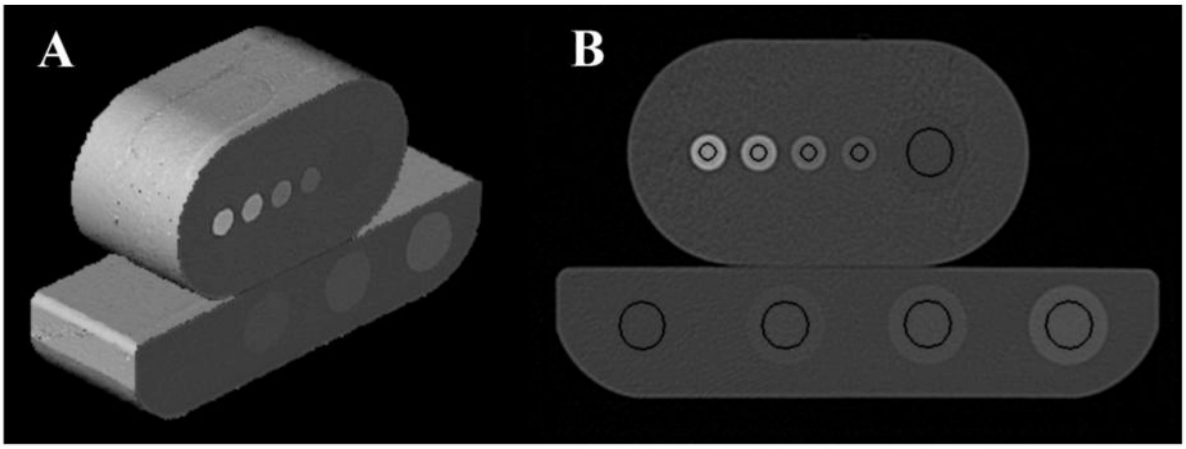

Figure 1.

Image Analysis calibration phantom (bottom) and medium-sized foot phantom with QRM inserts (top) are illustrated. A. shows a 3D rendering of the scanned portions. B. shows a cross-section through both phantoms and the circular regions of interest (black) for that slice that were used to measure attenuation in HUs. The ROI to the far left in the IA calibration phantom (bottom) is the “water” reference.

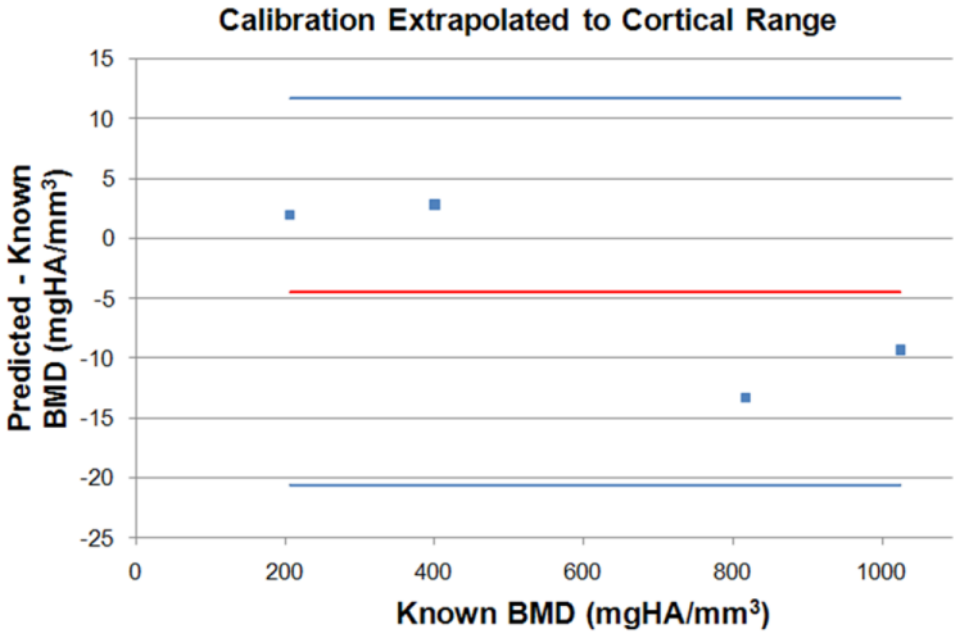

Figure 2.
Four QRM inserts, HA200, HA400, HA800, and HA1000 were scanned within the medium sized foot phantom. A Bland-Altman plot shows the known BMD values (as specified by QRM) compared to the predicted BMD values (IA BMD calibration curve extrapolated to the cortical range). The top and bottom horizontal lines represent the 95% limits of agreement about the mean (middle horizontal line).

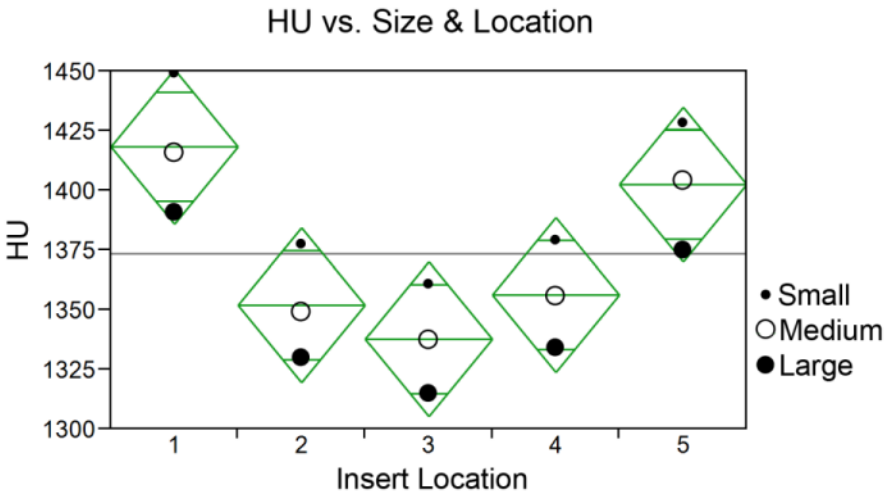

Figure 3.
Effects of foot phantom size and insert location on measured HU values. Location 3 is the innermost insert location. The horizontal line represents the grand mean and the tips of the diamonds represent the 95% confidence intervals. All locations contained PCTFE inserts.

Table 1

Effect of BMD calibration phantom in and out of the field of view.

QRM (mgHA/cm^3)	Measured (mgHA/cm^3)		% Difference	
	QRM w/ IA	QRM w/o IA	QRM w/ IA	QRM w/o IA
HA200 (206.4)	210.4±32.5	208.4±28.1	1.9	0.9
HA400 (400.2)	406.7±34.6	403.0±25.9	1.6	0.7
HA800 (816.3)	799.9±38.9	803.0±31.4	−2.0	−1.6
HA1000 (1024.1)	1001.1±50.0	1014.7±42.3	−2.2	−0.9

Values are given as Mean±Standard Deviation

Table 2

Effect of kVp relative to a 120 kVp baseline scan and to the QRM specified values.

QRM (mgHA/cm^3)	Measured (mgHA/cm^3)				% Difference	
	80 kVp	100 kVp	120 kVp	140 kVp	vs 120 kVp	vs QRM
HA200 (206.4)	208.6±30.2	208.0±27.5	208.4±28.1	208.2±27.4	0.0±0.1	0.9±0.1
HA400 (400.2)	393.5±31.4	397.3±27.5	403.0±25.9	403.2±28.2	−0.9±1.2	−0.2±1.2
HA800 (816.3)	798.0±34.9	798.7±30.4	803.0±31.4	800.7±31.3	−0.4±0.3	−2.0±0.3
HA1000 (1024.1)	1008.1±45.0	1009.1±42.9	1014.7±42.3	1012.2±42.6	−0.4±0.3	−1.3±0.3

Values are given as Mean±Standard Deviation

Table 3

Effect of table height relative to a scan at the isocenter and to QRM specified values.

QRM (mgHA/cm^3)	Measured (mgHA/cm^3)			% Difference	
	Isocenter	Middle	Low	vs 120 kVp	vs QRM
HA200 (206.4)	207.9±27.4	207.2±26.3	204.4±33.4	−1.0±0.9	0.0±0.9
HA400 (400.2)	398.3±26.8	396.6±26.1	391.2±37.1	−1.1±1.0	−1.2±0.9
HA800 (816.3)	797.1±30.9	803.7±31.9	794.1±39.5	−0.2±0.9	−2.2±0.6
HA1000 (1024.1)	1006.5±42.7	1013.8±43.0	1004.9±46.3	0.3±0.6	−1.5±0.5

Values are given as Mean±Standard Deviation

Table 4

Effect of reconstruction kernel on BMD.

QRM mgHA/cm^3	QRM mgHA/cm^3			
	B30f	**B35f**	**B40f**	**B70f**
HA0 (0.0)	−8.4.0±3.3	−8.1±3.1	−8.5±3.9	−8.9±23.5
HA200 (206.4)	222.7±4.3	213.5±4.1	222.0±5.1	209.4±29.6
HA400 (400.2)	423.9±5.1	406.3±4.6	422.7±6.0	405.7±27.5
HA800 (816.3)	847.5±7.7	814.2±6.1	844.6±8.6	799.0±31.7
HA1000 (1024.1)	1072.7±15.1	1029.3±12.6	1068.8±16.3	1010.4±45.1

Values are given as Mean±Standard Deviation